

# Nitrogen isotopes in the interstellar medium: A chemical journey across the Galaxy

Laura Colzi<sup>1,\*</sup>, Francesco Fontani<sup>2</sup>, Víctor M. Rivilla<sup>1</sup>, and Paola Caselli<sup>3</sup>

<sup>1</sup>Centro de Astrobiología (CAB), CSIC-INTA, Ctra. de Ajalvir Km. 4, 28850 Torrejón de Ardoz, Madrid, Spain

<sup>2</sup>INAF-Osservatorio Astrofisico di Arcetri, Largo E. Fermi 5, 50125 Florence, Italy

<sup>3</sup>Max-Planck-Institut für extraterrestrische Physik (MPE), Giessenbachstrasse 1, 85748 Garching, Germany

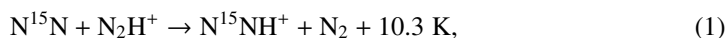
**Abstract.** One of the most important tools to investigate the chemical history of our Galaxy and our own Solar System is to measure the isotopic fractionation of chemical elements. This is the process that distributes the less abundant stable isotopes of an element in different molecules. The isotopic ratios are governed by two main processes: 1. chemical evolution of the whole Galaxy due to stellar nucleosynthesis; 2. local fractionation effects. In this Proceeding we report some results highlighting both processes towards massive star-forming regions.

## 1 Introduction

One of the main tools to understand the heritage that has been received by the Solar System is to study the isotopic variation. In fact, pristine Solar System materials, like comets and carbonaceous chondrites, present enrichment in <sup>15</sup>N and D, with respect to the proto-Solar Nebula (PSN) value (see e.g. the left panel of Fig. 1). This means that there was an alteration of isotopic ratios (e.g. the <sup>14</sup>N/<sup>15</sup>N ratio) during the Solar formation process, whose causes are still not well understood.

From an observational point of view the <sup>14</sup>N/<sup>15</sup>N ratio has been studied towards different type of molecular clouds, such as low-mass pre-stellar cores and protostellar objects, infrared dark clouds, massive star-forming regions, and protoplanetary discs (e.g. [2]; [3]; [4]; [5]; [6]; [7]; [8]; [9]), as shown in the right panel of Fig. 1. Most of the observed <sup>14</sup>N/<sup>15</sup>N ratios lie in between the cometary value (144±3, [10]) and the PSN value (441±6, [11]). However, there are also some exceptions, as the <sup>14</sup>N/<sup>15</sup>N ratios measured from N<sub>2</sub>H<sup>+</sup> towards pre-stellar cores and the ratios in some massive cores are even higher than the PSN value (e.g. [5]; [12]).

All of these different <sup>14</sup>N/<sup>15</sup>N ratios depending on the physical conditions of the sources and on the observed molecular species, raising interest also from a theoretical point of view. First, the so-called low-temperature isotopic-exchange reactions in chemical models have been invoked to explain the observed ratios (e.g. [13]; [14]; [15]), as:



which exchange one of the <sup>14</sup>N of N<sub>2</sub>H<sup>+</sup> with <sup>15</sup>N. These reactions are very efficient in a low-temperature environment (e.g. 5–10 K for pre-stellar cores, [16]) because of their exothermicities. Moreover, such reactions are also very successful in reproducing the D/H ratios

\*e-mail: lcolzi@cab.inta-csic.es

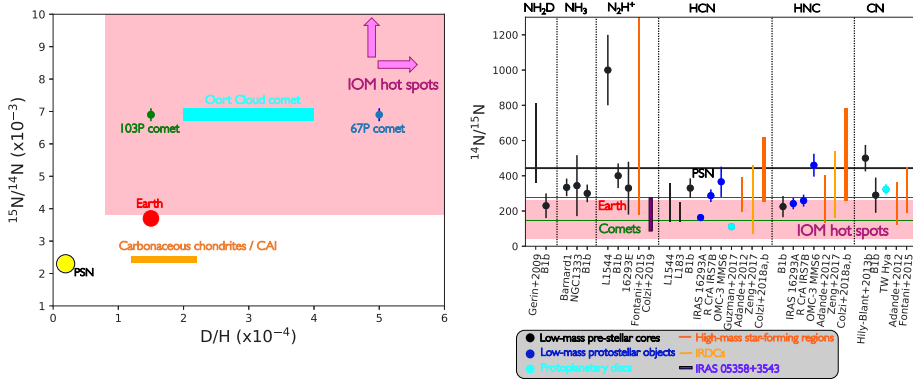


**Figure 1.** *Left panel:*  $^{15}\text{N}/^{14}\text{N}$  vs  $\text{D}/\text{H}$  in comets, chondrites, hot spots in the Insoluble Organic Matter (IOM) of meteorites, Earth and PSN. *Right panel:*  $^{14}\text{N}/^{15}\text{N}$  ratios obtained for different molecules. Black points represent low-mass pre-stellar cores, the blue points are low-mass protostellar objects, and the cyan points indicate protoplanetary discs. The horizontal yellow and red solid lines represent the PSN value of 441 and the terrestrial atmosphere value of 272, respectively. The green horizontal line denotes the average value measured in comets. The pink area represents measurements in carbonaceous chondrites, where the lower ones are the so-called "hot-spots". Adapted from [1].

in molecular clouds (e.g. [17]). However, this is not so for nitrogen fractionation. This indicates that there are other chemical processes that need to be taken into account. Other mechanisms, such as different rates for the dissociative recombination of  $\text{N}_2\text{H}^+$  (e.g. [15]), or the isotope-selective photodissociation of  $\text{N}_2$  (e.g. [18]) have been also proposed.

## 2 The role of the Milky Way chemical evolution

The  $^{14}\text{N}/^{15}\text{N}$  ratios are also governed by the chemical evolution of the whole Galaxy due to stellar nucleosynthesis (e.g. [19]). In this respect, we have analysed a sample of 87 massive star-forming regions observed with the IRAM 30m radiotelescope<sup>1</sup>. The sources span galactocentric distances,  $D_{\text{GC}}$ , from 2 up to 12 kpc allowing to study the  $^{14}\text{N}/^{15}\text{N}$  ratio of HCN and HNC as a function of  $D_{\text{GC}}$  (Fig. 2). For the two datasets we have performed a linear regression fit (light blue solid lines in Fig. 2) and a parabolic analysis (red parabolas in Fig. 2). From the linear trends we have derived a new local ISM  $^{14}\text{N}/^{15}\text{N}$  value of  $375 \pm 75$  ([9]). Then, the observational results have been compared with the predictions of the Galactic Chemical Evolution (GCE) model [19] (magenta lines in Fig. 2). They predict a linear positive trend up to 8 kpc because of novae outbursts as the main way to produce the  $^{15}\text{N}$ , and a flattening trend above this distance because of the low-level star formation and gas infall on long timescales (inside-out galaxy formation) that reduce the nova effect (see e.g. [19, 20]).

GCE models can reproduce the observational trend but not the absolute values. However, the shift on the y-axis of the models is defined by the ejected mass in the form of  $^{15}\text{N}$ ,  $M_{\text{eject}}^{15\text{N}}$ , which is an assumed parameter considering valid ranges taken from hydrodynamic simulations (see [19] for more details). More recent GCE models [20], which take into account different rotation velocities of low-metallicity massive stars, updated  $M_{\text{eject}}^{15\text{N}}$  and could better reproduce also the absolute value of observations.

We are now extending this trend towards the outer part of our Galaxy ( $D_{\text{GC}} > 12$  kpc), also updating GCE models with new stellar yields and approaching distances where CNO isotopes

<sup>1</sup>For more information on the observations and the analysis done see [8, 9].

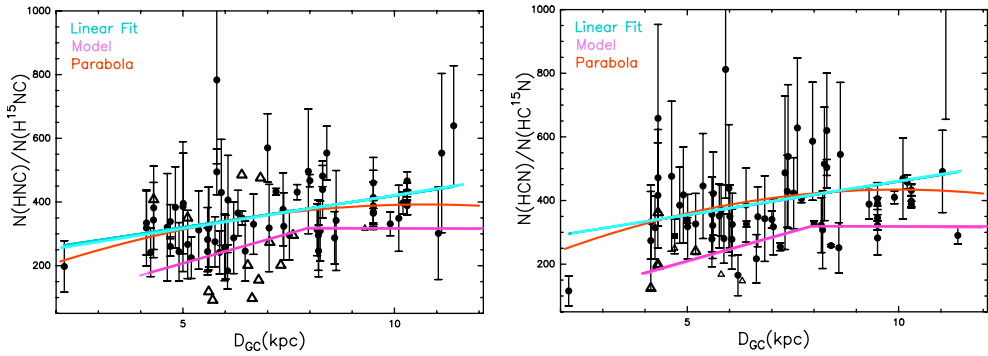


**Figure 2.**  $^{14}\text{N}/^{15}\text{N}$  ratios for HNC (*left panel*) and HCN (*right panel*) as a function of the galactocentric distance ( $D_{\text{GC}}$ ). The cyan solid line is the linear regression fit computed for the two data sets, the red parabola is the results from the parabolic analysis described in detail in [9], and the magenta solid line represents the GCE model of [19].

have never been studied (Colzi et al. in prep). In fact, this zone of the Galaxy present lower metallicities, a factor of four lower at  $D_{\text{GC}}=19$  kpc with respect to the inner Galaxy, which could also affect the behaviour of the elemental  $^{14}\text{N}/^{15}\text{N}$  ratio.

### 3 Local chemical fractionation effects

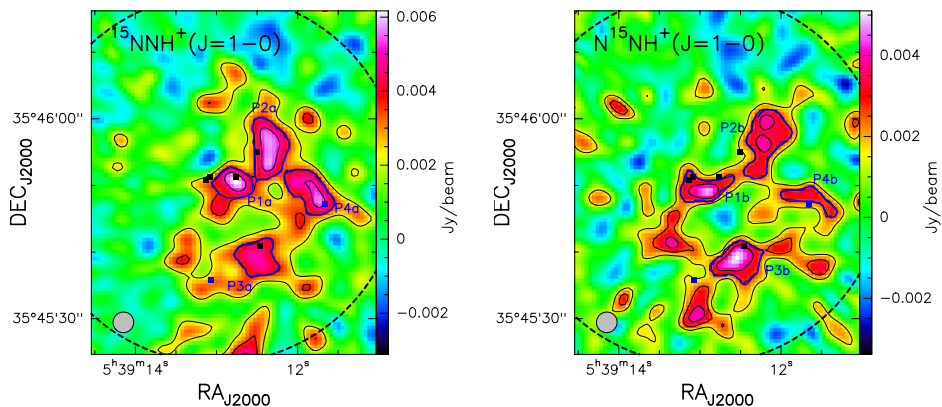


**Figure 3.** First interferometric maps of the  $J=1-0$  transition of  $^{15}\text{NNH}^+$  (*left panel*) and  $\text{N}^{15}\text{NH}^+$  (*right panel*). The black contour levels are 3, 5 and 7 times the  $1\sigma$  of the maps ( $0.5$  and  $0.72$   $\text{mJy beam}^{-1}$ , respectively). The blue contours correspond to the  $5\sigma$  of the map, from which the  $^{14}\text{N}/^{15}\text{N}$  ratios have been derived. The black and blue squares indicate the positions of the continuum sources and other  $\text{N}_2\text{H}^+$  peak positions, respectively. The dashed circle represents the NOEMA field of view and the synthesized beam is the ellipse indicated in the lower left corner.

To investigate the local effect of chemistry in individual star-forming regions we have studied for the first time N-fractionation of  $\text{N}_2\text{H}^+$  at high angular resolution ( $\sim 3''$ , i.e.  $\sim 6200$  au at a distance of 1.8 kpc). In particular, we have used IRAM NOEMA observations towards the massive star-forming region IRAS 05358+3543 ([21]).

Figure 3 shows the first interferometric maps of the  $^{15}\text{N}$ -isotopologues of  $\text{N}_2\text{H}^+$  at core scales (about 0.03 pc). From this work it appears that the  $^{14}\text{N}/^{15}\text{N}$  ratio of  $\text{N}_2\text{H}^+$  is lower in

the inner denser cores ( $\sim 100\text{--}200$ ) with respect to the more diffuse gas ( $>250$ ). These results highlight the importance of local fractionation effects, and in particular they demonstrates that isotope-selective photodissociation of  $\text{N}_2$  should be introduced in chemical models to explain  $^{15}\text{N}$ -enrichment in star-forming regions (e.g. [18]; [21]; [22]).

We have also obtained new NOEMA observations to study N-fractionation of the nitriles HCN and HNC towards the same source and with the same spatial resolution. The comparison of the  $^{14}\text{N}/^{15}\text{N}$  ratio of  $\text{N}_2\text{H}^+$  with that of nitriles will allow a deeper insight of the local chemical processes affecting isotopic ratios.

## References

- [1] L. Colzi, *Isotopic fractionation study towards massive star-forming regions across the Galaxy, PhD Thesis, Premio Tesi di Dottorato Series, Florence University Press* (2020)
- [2] F. Daniel, M. Gérin, E. Roueff, J. Cernicharo, N. Marcelino, F. Lique, D.C. Lis, D. Teyssier, N. Biver, D. Bockelée-Morvan, **560**, A3 (2013), 1309.5782
- [3] P. Hily-Blant, L. Bonal, A. Faure, E. Quirico, **223**, 582 (2013), 1302.6318
- [4] S.F. Wampfler, J.K. Jørgensen, M. Bizzarro, S.E. Bisschop, **572**, A24 (2014), 1408.0285
- [5] F. Fontani, P. Caselli, A. Palau, L. Bizzocchi, C. Ceccarelli, **808**, L46 (2015), 1506.05180
- [6] S. Zeng, I. Jiménez-Serra, G. Cosentino, S. Viti, A.T. Barnes, J.D. Henshaw, P. Caselli, F. Fontani, P. Hily-Blant, **603**, A22 (2017), 1705.04082
- [7] V.V. Guzmán, K.I. Öberg, J. Huang, R. Loomis, C. Qi, **836**, 30 (2017), 1701.07510
- [8] L. Colzi, F. Fontani, P. Caselli, C. Ceccarelli, P. Hily-Blant, L. Bizzocchi, **609**, A129 (2018), 1709.04237
- [9] L. Colzi, F. Fontani, V.M. Rivilla, A. Sánchez-Monge, L. Testi, M.T. Beltrán, P. Caselli, **478**, 3693 (2018), 1804.05717
- [10] P. Hily-Blant, V. Magalhaes, J. Kastner, A. Faure, T. Forveille, C. Qi, **603**, L6 (2017), 1706.10095
- [11] B. Marty, L. Zimmermann, P.G. Burnard, R. Wieler, V.S. Heber, D.L. Burnett, R.C. Wiens, P. Bochsler, **74**, 340 (2010)
- [12] E. Redaelli, L. Bizzocchi, P. Caselli, J. Harju, A. Chacón-Tanarro, E. Leonardo, L. Dore, **617**, A7 (2018), 1806.01088
- [13] E.S. Wirström, S.B. Charnley, M.A. Cordiner, S.N. Milam, **757**, L11 (2012), 1208.0192
- [14] E. Roueff, J.C. Loison, K.M. Hickson, **576**, A99 (2015), 1501.01141
- [15] J.C. Loison, V. Wakelam, P. Gratier, K.M. Hickson, **484**, 2747 (2019)
- [16] A. Crapsi, P. Caselli, M.C. Walmsley, M. Tafalla, **470**, 221 (2007), 0705.0471
- [17] P. Caselli, C. Ceccarelli, **20**, 56 (2012), 1210.6368
- [18] K. Furuya, Y. Aikawa, **857**, 105 (2018), 1803.06787
- [19] D. Romano, F. Matteucci, Z.Y. Zhang, P.P. Papadopoulos, R.J. Ivison, *Monthly Notices of the Royal Astronomical Society* **470**, 401 (2017), 1704.06701
- [20] D. Romano, F. Matteucci, Z.Y. Zhang, R.J. Ivison, P. Ventura, *arXiv e-prints arXiv:1907.09476* (2019), 1907.09476
- [21] L. Colzi, F. Fontani, P. Caselli, S. Leurini, L. Bizzocchi, G. Quaiá, **485**, 5543 (2019), 1903.06567
- [22] A.N. Heays, R. Visser, R. Gredel, W. Ubachs, B.R. Lewis, S.T. Gibson, E.F. van Dishoeck, **562**, A61 (2014), 1401.1630